Ph.D. Thesis

Combined effects of melatonin and FGF-2 on mouse osteoblast (MC3T3-E1) behavior within IP-CHA constructs – *in vitro* analysis

MOHAMMAD ZESHAAN RAHMAN

Department of Oral and Maxillofacial Surgery,

Graduate School of Biomedical and Health Sciences,

Hiroshima University

Supervisor: Masaaki Takechi, D.D.S., Ph.D.

2016

APPROVAL SHEET

As member of dissertation committee, we certify that we have read the dissertation

Prepared by: Mohammad Zeshaan Rahman

Entitled: **COMBINED EFFECTS OF MELATONIN AND FGF-2 ON MOUSE OSTEOBLAST (MC3T3-E1) BEHAVIOR WITHIN IP-CHA CONSTRUCTS – *IN VITRO* ANALYSIS**

and recommend that it be accepted as fulfilling the dissertation requirement for the degree of Doctor or Philosophy (Ph.D.) from Hiroshima University, Japan.

STATEMENT BY THE AUTHOR

I declare that this dissertation represents my own academic work, except where due acknowledgment is made. This dissertation has not previously been included in any thesis dissertation or report submitted to this University or any other University for the award of a degree.

Mohammad Zeshaan Rahman.

Date:

AKNOWLEDGEMENT

Foremost, I would like to express my gratitude to my advisors, Professor Nobuyuki Kamata and Professor Motoyuki Sugai for allowing me to be a part of the Department of Oral and Maxillofacial Surgery and carry out my research at Hiroshima University.

I would take this opportunity to sincerely thank my Associate Professor Masaaki Takechi who supervised my research and helped me complete my Ph.D. degree. His support as an advisor, mentor and guide helped me as a foreign student both in my academic and personal life in Japan. His prompt attitude towards my quarries helped me overcome the difficulties of being a foreign student.

I would like to express my gratitude to Hideo Shigeishi for transforming a dentist like myself into an accomplished researcher and Dr. Akira Ota for everything else. I would also like to extend my gratitude to my advisor committee, Professor Koichi Kato, Professor Masaru Sugiyama and Professor Kazuhiro Tsuga without whom this dissertation could not have been complete.

I would like to sincerely thank Otsuka Toshimi Scholarship Foundation for allowing me to concentrate on my research while taking care of my financial requirements. I would like to thank Grant-in-Aid for Scientific Research(C) from the Ministry of Education, Culture, Sports, Science and Technology, Japan. (No.23592993).

I would like to express my appreciation to my mother, Zarine Tilat, my father Dr. Kazi Rahman and especially my wife Tahsin Raquib Abonti for standing by my side inspite of her

own Ph.D. research and dessertation, my beloved son, Ayaaz Rahman who helped me overcome the monotonous life of a postgraduate student.

At last I would like to dedicate my research and all my academic endeavors to my country, Bangladesh for giving me the identity and the ability to represent myself in the world stage. I shall forever be indebted to provide my best to the people of Bangladesh. My family, my country and I would forever be grateful to Hiroshima University and Japan for giving me the knowledge and competence – 誠にありがとうございました.

Table of Content

ABSTRACT

Biocompatible materials such as interconnected porous calcium hydroxyapatite (IP-CHA) loaded with osteogenic cells and bioactive agents are part of an evolving concept for overcoming craniofacial defects by use of artificial bone tissue regeneration. Amongst the bioactive agents, melatonin (MEL) and basic fibroblast growth factor (FGF-2) have been independently reported to induce osteoblastic activity. The present *in vitro* study was undertaken to develop a model for cell seeding into the IP-CHA construct as model for future study and also understand the combinatory relationship of the two bioactive agents (FGF-2 and MEL) on osteoblastic activity and mineralization *in vitro*. Mouse preosteoblast cells (MC3T3-E1) were seeded and cultured within cylindrical type of IP-CHA block (ø4 X 7mm) in four different methods – Static, Centrifugation, Agitation and Vacume-assisted. Based on proliferation assay and alkaline phosphatase enzyme activity, the vacume-assisted cell-seeding method yielded significantly good results. Next, the optimum concentration of FGF-2 and MEL was determined by subjecting the IP-CHA/MC3T3 composites to varying concentration of FGF-2 (2, 20 and 100µg/ml) and MEL (50, 200 and 1000nM). 20µg/ml of FGF-2 and 200nM of MEL were used as the optimum concentration for your study based on our findings of mRNA expressions. The combination of FGF-2 and MEL showed significantly increased osteoblastic activity in terms of proliferation, alkaline phosphatase enzyme and mRNA expressions. The combination also showed augmented stains of mineralization on MC3T3-E1 cells, both in monolayer cultures as well as within IP-CHA. These findings indicate that the combination of FGF-2 and MEL may be utilized with biocompatible materials to attain augmented osteogenic activity and mineralization.

INTRODUCTION

Bone grafting plays an essential role in craniofacial surgery performed for both reconstructive and aesthetic purposes, which has led to discovery of different biomaterials, including hydroxyapatite (HAp), a member of the non-resorbable calcium phosphate group of biomaterials[1]. HAp has been formed into a variety of shapes and dimensions, and shown both biocompatibility and osteoconductivity since the discovery of its similarities with natural bone[2]. Porous type HAp ceramics are expected to facilitate bone formation and become integrated with host bone tissue. However, the pores of HAp are not fully replaced with new bone for a substantial period of time due to limited interconnection, which eventually leads to undesirable results[3]. The interconnection of pores is considered to be an essential factor for osteoconduction inside a HAp ceramic appliance for cell viability and function. To overcome this problem, interconnected porous calcium HAp ceramic (IP-CHA) components with fully interconnected and symmetrical pores have been developed[4]. This unique structure provides extensive incorporation with host cells more rapidly than other types of porous calcium HAp ceramic, while its porous architecture also provides optimum compressive strength of up to 12 MPa, similar to cancellous bone.[5]. It has been suggested that IP-CHA may have an additional osteoinductive advantage if the porous architecture could be utilized to transplant osteoinductive agents or osteogenic cells or both[6]. In our previous study, we showed eminent bone formation with both granular and block type IP-CHA[7].

Melatonin (MEL) is a pineal hormone that is also synthesized from other human cells and organs, such as the retina[8], bone marrow[9], platelets[10], gastrointestinal tract[11], skin[12], and lymphocytes[13]. Roth et al. demonstrated the direct effects of MEL on differentiation of rat pre-osteoblast cells[14], while it has also been reported to inhibit RANKL-induced bone

resorption and thereby promote bone formation[15]. These observations imply that MEL positively influences bone formation.

Fibroblast growth factor 2 (FGF-2) is a versatile member of the 23-polypeptide growth factor family. It has been found to participate in a variety of biological processes, such as angiogenesis[16], embryonic development[17], hematopoiesis[18], and cardiac muscle[19] and bone[20] development. In addition, the presence of FGF-2 in skeletal tissue suggests its role in bone remodeling and *in vitro* findings have shown that it positively regulates bone formation[21]. Furthermore, FGF-2 has been reported to stimulate osteoblast proliferation in immature cells rather than differentiation[22].

Even though both MEL and FGF-2 play significant roles in bone formation, their combined effects on osteoblast activity and bone formation have not been reported. Also, their combination within useful biomaterials, such as HAp, remains undocumented. Here, we investigated the effects of FGF-2 and MEL in combination on rat osteoblast cells when cultured within an IP-CHA construct.

MATERIAL & METHODS

Cell culture

MC3T3-E1 mouse pre-osteoblast cells were cultured in α-minimal essential medium (α-MEM) (Gibco) supplemented with 10% fetal bovine serum (FBS; Gibco), 1% penicillin-streptomycin, and L-Glutamate, and incubated with 5% CO_2 at 37^{o}C.

IP-CHA Construct

We used a cylindrical type of porous IP-CHA block (NEOBONE® MTT, Japan) that was 7 mm in diameter, 4 mm in height, with 75% porosity (Figure 1). The mean porous diameter was 150 µm and the porous interconnections were 40 µm. Prior to cell seeding, IP-CHA blocks were pre-coated with cell-free medium to enhance cell adhesion in the interior of the scaffold. Medium was trickled onto the block and then it was subjected to a vacuum, which moved the air out of the porous IP-CHA and drew medium in.

Determination of the most efficient cell seeding method

Once the monolayer cells were sub-confluent, viability was determined by trypan blue staining. Next, $1x10^5$ viable cells were resuspended in 130 µl of expansion medium and concentrated cell suspensions were pipetted onto the IP-CHA in a 24-well plate as follows,

Static Cell Seeding: For static seeding, 130 µl of concentrated cell suspensions was pipetted onto IP-CHA blocks.

Centrifugation Cell Seeding: For centrifugation cell seeding method, IP-CHA block were placed in plastic tube along with $1X10^5$ concentrated cell suspension and centrifuged at 2000 rpm (16000g) for 3 mins. Re-suspension was carried at 1 min interval[23].

Agitation Cell Seeding: For agitation method, concentrated cell suspension along with IP-

CHA block was continuously agitated at 200 rpm (1600g) at 37^{o}C for 2 hours[24].

Vacume-assisted Cell Seeding: For vacuum-assisted method, concentrated cell suspension containing 1X10^{5} cells were pipetted onto IP-CHA blocks and subjected to vacuum condition (100mmHg) for 100ms[25].

After substantial cell seeding, an additional 1.5 ml of expansion medium was added later to the IP-CHA/MC3T3 composites. All the samples were incubated for upto 3 days with 5% CO_2 at 37^{o}C to aid proliferation within the scaffold before treating and evaluating the seeded cells.

Cell proliferation assay

Cell proliferation with different cell seeding methods was evaluated using an MTS Assay (Aqueous One Cell Proliferation Assay, Promega, Madison, WI) after 3 days. The principal behind the MTS assay is the formation of formazan crystals by dehydrogenase enzyme in functionally active cell mitochondria. The amount of purple formazan formed is directly proportional to the number of viable cells. The method was performed according to the manufacturer's protocol. Briefly, the IP-CHA/MC3T3 composite were gently rinsed in PBS and transferred to a new 24-well plate. MTS solution (100 µl per 1 ml of expansion medium) was added to the composites and subjected to a vacuum at 100 mmHg for 100 milliseconds to ensure that the MTS solution entered the core. Next, the composite was allowed to incubate for 2 hours, after which the medium in the well was gently aspirated and discarded. Finally, 750 µl of dimethyl sulfoxide was added for dissolving the formazan crystals formed by the cells within the composite and 250 mL of this solution was transferred to a 96-well plate, and absorbance at 490 nm was measured using a microplate reader (Bio-Rad, Bio-Rad Laboratories, Inc. CA, USA). Results are expressed as the mean ± SD of 3 independent experiments.

ALP Assay

For the different cell seeding methods, ALP enzyme activity was determined using an ALP assay measurement kit (TRACP & ALP Assay Kit, Takara Bio Inc. Japan). After 3 days of incubation in normal culture medium, the IP-CHA/MC3T3 composites were transferred to osteogenic induction medium (∂-MEM supplemented with ß-glycerophosphate and ascorbic acid). After 5 and 7 days of incubation the samples washed 3 times in PBS, then homogenized in the provided extraction solution and sonicated for 3 minutes. Cell lysates were then collected by centrifugation for 5 minutes and 50µl of the supernatant was mixed with 50µl of the substrate solution provided in the assay kit. The solution was then incubated at 37°C for 1 hour before measuring absorbance at 405 nm (Bio-Rad, Bio-Rad Laboratories, Inc. CA, USA). Results are expressed as the mean ± SD of 3 independent experiments.

FGF-2 treatment

Mouse recombinant FGF-2 (Sigma-Aldrich) was used to evaluate the optimum concentration of FGF-2 needed for cell proliferation; therefore the samples were subjected to different concentrations of FGF-2 (2, 20, 100 µg/ml).

MEL treatment

MEL (Sigma-Aldrich) was used to evaluate the optimum concentration of MEL needed for cell differentiation; therefore the samples were subjected to different concentrations of MEL (50, 200, 1000 nM).

RNA extraction and RT-PCR method

RNA was extracted using an RNAeasy micro kit (Qiagen). Reverse transcription into cDNA was performed using SuperScript III First Strand Synthesis Supermix (Invitrogen). Quantification of mRNA levels was carried out using Eppendorf Master Cycler and SYBR

Green Master Mix (TOYOBO, Tokyo, Japan). The reaction mixture consisted of 1.0 µg of cDNA, 12 µl of SYBR Green Mix, and 10 µmol of each pair of oligonucleotide primers. GAPDH was used as the reference mRNA control. The RT PCR was made to run in agrose gel electrophoresis using 10µl of PLUS DNA LADDER and 1µl of 10X Loading Buffer at 100V for 20minutes. The primer sequences were: COL-1; 5'- -3' (sense), 5'- -3' (antisense), ALP; 5'- -3' (sense), 5'- -3' (antisense), OPN; 5'- -3' (sense), 5'- -3' (antisense), OCN; 5'- -3' (sense), 5'- -3' (antisense), and G3PDH; 5'- -3' (sense), 5'- -3' (antisense). The real time PCR protocol was as follows: initial melting at 95^{o}C for 10 minutes, followed by 40 cycles at 95^{o}C for 15 seconds, 60^{o}C for 30 seconds, and 72^{o}C for 40 seconds. Reverse transcribed Human Total Reference RNA (Stratagene, Cheshire, UK) was used to plot a standard curve. Results are expressed as the mean ± SD of 3 independent experiments.

Cell proliferation with FGF-2 and/or MEL treatment

Cell proliferation with FGF-2 and/or MEL treatment was evaluated using an MTS Assay (Aqueous One Cell Proliferation Assay, Promega, Madison, WI) after 1, 3, and 5 days. The principal behind the MTS assay is the formation of formazan crystals by dehydrogenase enzyme in functionally active cell mitochondria. The amount of purple formazan formed is directly proportional to the number of viable cells. The method was performed according to the manufacturer's protocol. Briefly, the IP-CHA/MC3T3 composite was treated with and without FGF-2 and/or MEL, then gently rinsed in PBS and transferred to a new 24-well plate. MTS solution (100 µl per 1 ml of expansion medium) was added to the composite and subjected to a vacuum at 100 mmHg for 100 milliseconds to ensure that the MTS solution entered the core. Next, the composite was allowed to incubate for 2 hours, after which medium in the wells was gently aspirated and discarded. Finally, 750 µl of dimethyl sulfoxide was added for dissolving the formazan crystals formed by the cells in the composite and 250 mL of this solution was transferred to a 96-well plate, and absorbance at 490 nm was

measured using a microplate reader (Bio-Rad, Bio-Rad Laboratories, Inc. CA, USA). Results are expressed as the mean ± SD of 3 independent experiments.

ALP Assay for the IP-CHA/MC3T3 composites

ALP enzyme activity was determined using an ALP assay measurement kit (TRACP & ALP Assay Kit, Takara Bio Inc. Japan). Briefly, the IP-CHA/MC3T3 composites after 3, 5, and 7 days of culture with FGF-2 and/or MEL were washed 3 times in PBS, then homogenized in the provided extraction solution and sonicated for 3 minutes. Cell lysates were then collected by centrifugation for 5 minutes and 50µl of the supernatant was mixed with 50µl of the substrate solution provided in the assay kit. The solution was then incubated at 37°C for 1 hour before measuring absorbance at 405 nm (Bio-Rad, Bio-Rad Laboratories, Inc. CA, USA). Results are expressed as the mean ± SD of 3 independent experiments.

Alizarin Red staining for the extracellular calcium deposits

Extracellular calcium deposits were examined by Alizarin Red staining. Briefly, Alizarin Red solution was freshly prepared by dissolving 2 g of Alizarin Red (SIGMA) in 100 ml of deionized distilled water, then pH was incrementally adjusted to 4.1-4.3 using 0.1% NH_4OH solution. The monolayer cultures were gently washed with PBS. The cells were fixed in enough 10% neutral buffered formalin (SIGMA) to submerge the cells. After 30 minutes, formalin was gently aspirated and the cells were washed with deionized distilled water. Finally, prepared Alizarin Red solution was added to cover the cells and incubated at room temperature in the dark for 45 minutes, after which the monolayer cells were examined under a microscope.

Alizarin Red Quantification

Extracellular calcium deposits in cells cultured within IP-CHA constructs were examined by

Alizarin Red staining. Briefly, Alizarin Red solution was freshly prepared by dissolving 2 g of Alizarin Red (SIGMA) in 100 ml of deionized distilled water, then pH was incrementally adjusted to 4.1-4.3 using 0.1% NH_4OH solution. The treated IP-CHA/MC3T3 composites were gently washed with PBS. The cells were fixed in enough 10% neutral buffered formalin (SIGMA) to submerge the composite. After 30 minutes, formalin was gently aspirated and the cells were washed with deionized distilled water. Finally, prepared Alizarin Red solution was added to cover the composites and put into a vacume to allow the Alizarin Red solution to be drawn into the construct. It was then further incubated at room temperature in the dark for 45 minutes, after which the IP-CHA/MC3T3 composites were quantified. Briefly, the monolayers and treated IP-CHA/MC3T3 composites were submerged in 20% methanol and 10% acetic acid solution in water for quantification. After substantial vortexing, readings were obtained using a spectrophotometer at 450 nm of absorbance. Results are expressed as the mean ± SD of 3 independent experiments.

RESULTS

EXPERIMENT 1: MOST EFFICIENT CELL SEEDING METHOD.

Experiment 1.1: Proliferation Assay

In **Figure 2**, amongst the 3 methods used in our study, vacume-assisted cell seeding method showed significantly more proliferation compared to the static, agitation and centrifugation methods. The reason for this could be due to the fact that the vacume-assisted method harbored more cells compared to the other methods.

Experiment 1.2: .ALP Assay

In **FIGURE 3,** the data shows that compared to the static method the vacume-assisted method showed significant higher alkaline phosphatase activity. Amongst the 4 methods of cell seeding, the vacume-assisted showed greater alkaline phosphatase enzyme activity, which we believe, might be due to the larger number of cells adhering to the interior of the IP-CHA construct.

EXPERIMENT 2: OPTIMUM CONCENTRATION DETERMINATION OF FGF-2 AND MEL

Experiment 2.1: FGF-2 treatment

FGF-2 significantly induced Collagen 1 **(COL-1)** (Figures 4) and Alkaline Phosphatase **(ALP)** (Figure 5) mRNA expression at 20 µg/ml compared to the control and 2µg/ml. The lowest concentration that can elicit an osteoblastic response could therefore be considered

20μg/ml for our study. Student's t-test statistical significances of $P<0.05$ and $P<0.01$ were indicated by *, ** respectively.

Experiment 2.2: MEL treatment

Melatonin significantly induced Osteopontin **(OPN)** (Figure 6) and Osteocalcin **(OCN)** (Figure 7) mRNA at 200nM compared to the control and 50nM treatment. The lowest concentration that can elicit an osteoblastic response could therefore be considered 200nM for our study. Student's t-test statistical significances of $P<0.05$ and $P<0.01$ were indicated by *, ** respectively.

EXPERIMENT 3: COMBINED EFFECT OF MEL AND FGF-2 ON OSTEOBLASTIC ACTIVITY

Experiment 3.1 Combined Effect Of MEL And FGF-2 On Proliferation Assay

To evaluate the combined effect of FGF-2 and MEL on the proliferative potential of MC3T3-E1 cells within an IP-CHA construct, IP-CHA/MC3T3-E1 composites were examined in the presence of 20 μg/ml FGF-2 and/or 200 nM MEL after 1, 3, and 5 days of culture. FGF-2 independently and significantly induced growth of MC3T3-E1 cells as compared to the control on day 5 (Figure 8), whereas MEL alone did not show a significant effect on cell proliferation. Moreover, the MEL did not interfere with the proliferative potential of FGF-2.

Experiment 3.2 Combined Effect of MEL and FGF-2 on mRNA Expressions of Late Osteogenic Marker

OPN and OCN are considered to be late osteogenic markers, having roles in the onset of the mineralization phase of osteoblast lineage[26]. Figure 8 shows OPN and OCN mRNA expressions. Individual treatment by FGF-2 and MEL induced expression of these markers

from day 5, though MEL treatment had a more significant effect (Figure 9) compared to the FGF-2. On the other hand, combined treatment had an even greater effect on increased OCN and OPN expression (Figure 9).

Experiment 3.3 Combined Effect of MEL and FGF-2 on Alkaline Phosphatase Enzyme Activity

Figure 10 shows the relative ALP enzyme activities of MC3T3-E1 cells cultured within IP-CHA constructs with MEL and/or FGF-2 on days 3, 5, and 7. ALP enzyme activity is known to be closely associated with osteoblast differentiation. Both FGF-2 and MEL independently induced ALP activity from day 3, though that by the latter was more prominent (Figure 10). The combination resulted in significantly greater ALP enzyme activity as compared to the individual treatments (Figure 10).

EXPERIMENT 4.1: COMBINED EFFECT OF MEL AND FGF-2 ON MINERALIZATION IN MONOLAYER CULTURES.

Experiment 4.1 Combined Effect of MEL and FGF-2 on Mineralization in Monolayer Cultures. (Alizarin Red Staining)

The alizarin red staining of the monolayer cultures shows increased stains of mineralization after 2 weeks of treatment with the MEL, FGF-2, in osteogenic induction medium compared to the control (Figure 11). Both MEL and FGF-2 independently show mineralization but the combination of MEL and FGF-2 showed more intense stains of mineralization (Figure 11).

Experiment 4.2 Combined Effect of MEL and FGF-2 on Mineralization within IP-CHA/MC3T3 composites (Alizarin Red Quantification)

The quantification of the alizarin red stained cells within IP-CHA construct shows increased

mineralization after 2 weeks of treatment with the MEL and/or FGF-2, in osteogenic induction medium compared to the control. Compared to control and FGF-2, mineralization can been seen in lone treatment by MEL but the combination of MEL and FGF-2 showed significantly higher mineralization (Figure 12).

OVERVIEW OF THE RESULTS

The general osteoblast lineage is comprised on an initial proliferation phase, followed by a matrix maturation phase and ends with a mineralization phase (Figure 13). Our study was designed to illustrate the effect of our bioactive agents, FGF-2 and MEL on the different phases of bone lineage. The Proliferation assay, ALP assay, mRNA expression and Alizarin Red Staining with quantification was conducted to show the proliferation phase, the matrix maturation phase, the beginning of mineralization phase and mineralization phase respectively[26] (Figure 13).

Our results showed that FGF-2 mainly induces proliferation whereas MEL mainly induces the late osteogenic differentiation markers and influences the start of mineralization. The combination of MEL and FGF-2 shows increased expression of late bone markers, increased ALP enzyme activity and more intense stains of mineralization both in monolayer cultures and within IP-CHA constructs.

DISCUSSION

Fully interconnected and symmetrically porous IP-CHA has been suggested as a suitable candidate for transplantation of osteoinductive agents and/or osteogenic cells. HAp is a generally biocompatible material and possesses the advantage of protein adhesion whereby it can facilitate cell binding, proliferation, and differentiation, leading to matrix organization[27]. The high-energy substrata on the surface of HAp also make it a suitable candidate for initial cell attachment[28]. The IP-CHA blocks in our study had an average interconnection size of 40 μm, which is suitable for optimum cell metabolism within constructs in the context of an average mammalian nucleus being over 10 μm[29]. Attachment of MC3T3-E1 cells to porous hydroxyapatite was well-documented in a study presented by Smith et al[30]. Furthermore, Webster et al. suggested that the hydrophilicity of scaffolds increased the adhesion of MC3T3-E1 cells[31], which may explain the affluent attachment of MC3T3 cells when cultured within IP-CHA along with its wettability.

FGF-2 was reported to induce the growth of MC3T3-E1 cells in a study that validated its role in osteoblast proliferation[32]. Also, a number of studies have shown the relationship between bone formation and FGF-2 using the Wnt signaling pathway[33]. FGF-2 has been reported to increase N-cadherin expression, which enhances cell-cell adhesion in human calvaria osteoblasts[34], thus providing proper communication between adjacent cells. Zivko M et al. also suggested that gap junctional communication between adjacent cells is key to effective cell proliferation, growth, and differentiation at the cell-biomaterial interface[35]. Therefore, the use of FGF-2, as in our study, may be beneficial for cellular activity within an IP-CHA construct.

Bone formation is a cascade of events that occur in the initial proliferation phase,

followed by the mineralization phase marked by OPN and OCN expressions[26]. FGF-2 has been reported to be an eminent growth factor more favorable to cell proliferation than differentiation[36], which was also shown in our study using IP-CHA constructs. This phenomenon is of particular interest, because FGF-2 significantly increased the osteoblast population within the IP-CHA constructs in our study, ensuring that more cells were available for entering the maturation phase of bone formation.

The role of MEL on bone metabolism is well documented, and its potential for differentiation and mineralization in the absence of ascorbic acid or conventional osteogenic induction medium using pre-osteoblastic (MC3T3-E1) and osteoblast-like cells was shown[16]. The pathway responsible for osteogenic differentiation has been identified as BMP/ERK/Wnt[34]. Furthermore; MEL has been reported to positively stimulate bone formation by suppressing RANKL-mediated osteoclast formation and resultant bone resorption in the bone remodeling cycle[37]. The ability of bone marrow cells to synthesize and present ME (100 times higher than that in rat serum) suggest that MEL may have a local regulatory effect on bone[38]. MEL is also believed to influence calcium metabolism, which indirectly influences parathyroid activity, and controls the secretion of calcitonin and prostaglandins, thereby influencing bone metabolism[39]. Although MEL did not significantly influence the rate of cell growth in our study, as anticipated, its differentiation potential was largely highlighted by the mRNA expressions of the late bone markers OPN and OCN. MEL also induced mineralization, as shown by Alizarin Red staining. These findings suggested that the impact of MEL is more inclined towards the differentiation phase of osteoblast lineage.

MEL may induce increased cellular activity and differentiation because of its activity as an inherent free radical scavenger[40]. MC3T3 cells expel various free radicals during proliferation and growth[41], while buildup of a large amount of free radicals hampers the natural activity of MC3T3 cells, leading to inhibition of mineralization[42]. Therefore, we speculate that MEL assists MC3T3 cellular activity and mineralization by neutralizing free

radicals. In the present study, the combination of FGF-2 and MEL unregulated OPN and OCN, and also increased mineralization as compared to treatment with each alone. We concluded that FGF-2 induces proliferation, which provides a larger number of cells for MEL to induce to differentiate into mature osteoblasts and therefore positively regulate mineralization.

FGF-2 was previously studied in combination with other growth factors, such as bone morphogenic proteins (BMPs), and shown to significantly stimulate cell proliferation, while BMPs alone significantly stimulated differentiation and in combination with FGF-2 increased mineralization[43]. The combination of MEL and FGF-2 in the present study may operate in a similar manner, in which FGF-2 acts as the proliferative agent and MEL as the differentiating agent. This finding may also help to consider delayed administration of MEL in a future *in vivo* model. We found that MEL induced differentiation of pre-osteoblasts into mature bone forming successors. These findings may help explain the findings presented by Takechi et al., in which superior osseointegration was achieved by use of titanium screws in rat tibias after systemic administrations of MEL and FGF-2[44].

CONCLUSIONS

In conclusion, the vacume-assisted cell seeding method is an efficient way of seeding cells within IP-CHA constructs for in-vitro study. FGF-2 and MEL may play a significant synergistic role to enhance osteoblastic activity and mineralization of MC3T3-E1 cells within IP-CHA constructs by targeting different phases of the osteoblast lineage. Clinically, combined use of FGF-2 and MEL may be a reasonable adjunct to biomaterials for use in eminent craniofacial surgery.

REFERENCES

1. Osborn JF, Newesely H: The material science of calcium phosphate ceramics. J. Biomaterials 1980, 1:108-111
2. Woodard JR, Hilldore AJ, Lan SK, Park CJ, Morgan AW: The mechanical properties and osteoconductivity of hydroxyapatite bone scaffold with multi-scale porosity. Biomaterials 2007, 28: 45-54
3. Ayers RA, Simske SJ, Nunes CR, Wolford LM: Long-term bone ingrowth and residual micro hardness of porous block hydroxyapatite implants in humans. J Oral Maxillofac Surg 1998, 56: 1297-1301
4. Tamai N, Myoui A, Kudawara I, Ueda T, Yoshikawa H: Novel fully interconnected porous hydroxyapatite ceramic in surgical treatment of benign bone tumor. Journal of Orthopaedic Science : Official Journal of the Japanese Orthopaedic Association 2010, 15(4): 560–8.
5. Tamai N, Myoui A, Tomita T, Nakase T, Tanaka J: Novel hydroxyapatite ceramics with an interconnective porous structure exhibit superior osteoconduction in vivo. J Biomed Mater Res 2002, 59:110-117
6. Yoshikawa H: Bone tissue engineering with porous hydroxyapatite ceramics. J Artif Organs. 2005, 8:131-136
7. Minami M, Takechi M, Ohta K, Ohta A: Bone formation and osseointegration with titanium implant using granular- and block-type porous hydroxyapatite ceramics (IP-CHA). Dent Mater J. 2013, 32(5):753-60.
8. Liu C, Kukuhara C, Wessel JH III, Iuvone PM: Localaization of Aa-nat mRNA in the rat retina: melatonin synthesis by florescence in situ hybridization and laser capture microdissection. Cell Tissue Res 2004, 315: 197-201.

9. Conti A, Conconi S, Hertens E, Skwarlo-Sonta K, Markowska M: Evidence for melatonin synthesis in mouse and human bone marrow cells, J Pineal Res 2000, 28: 193-202
10. Champier J, Llaustrat B, Besancon R, Eymin C, Killer C: Evidence for tryptophan hydroxylase and hydroxyindo-O-methyl-transferase mRNAs in human blood platelets. Life Sci 1997, 60: 2191-2197.
11. Bubenik GA: Gastrointestinal melatonin: localization, function and clinical relevance. Dig Dis Sci 2000, 47: 2336-2348.
12. Slominski A, Fischer TW, Zmijewski MA, WOrtsman J, Semak I: On the role of melatonin in skin physiology and pathology. Endocrine 2005, 27: 137-148.
13. Carillo-Vico A, Calvo JR, Abreu P, Lardone PJ, Garcia-Maurino S: Evidence of melatonin synthesis by human lymphocytes and its physiological significance: possible role as intracrine, autocrine and/or paracrine substance. FASEB J 2004, 18: 537-539.
14. Roth J, Lin, W. L., & Cho, M. I: Melatonin promotes osteoblast differentiation and bone formation. The Journal of Biological Chemistry 1999 274(31): 22041–7.
15. Zofia O, Katarzyna Z, Beata K, Elżbieta Ś: Melatonin, the RANKL / RANK / OPG system, and bone metabolism in girls with anorexia nervosa. J Endocrinology 2010 61(1): 117–123.
16. Parsons-Wingerter, P, Elliott KE, Clark J: Fibroblast Growth Factor-2 Selectively Stimulates Angiogenesis of Small Vessels in Arterial Tree. Arteriosclerosis, Thrombosis, and Vascular Biology, 2000 20(5): 1250–1256.
17. Thisse B, Thisse C: Functions and regulations of fibroblast growth factor signaling during embryonic development. Developmental Biology, 2005, 287(2): 390–402.
18. Krejci P, Faitova J, Laurell H, Hampl A, Dvorak P: FGF-2 expression and its action in human leukemia and lymphoma cell lines. Leukemia 2003, 17(4): 818–20.

19. Detillieux KA, Sheikh F, Kardami E, Cattini P: Biological activities of fibroblast growth factor-2 in the adult myocardium. Cardiovascular Research 2003, 57(1): 8–19.
20. Burgess WH, Maciag T: The heparin-binding (fibroblast) growth factor family of proteins. Annu Rev Biochem 1989, 58:575-606
21. Canalis E, Centrella M, Mccarthy T: Effects of Basic Fibroblast Growth Factor on Bone Formation In Vitro Collagen degradation. J Clin Invest 1988, 81: 1572-1577
22. Mansukhani A, Bellosta P, Sahni M, Basilico C: Signaling by fibroblast growth factors (FGF) and fibroblast growth factor receptor 2 (FGFR2)-activating mutations blocks mineralization and induces apoptosis in osteoblasts. The Journal of Cell Biology 2000, 149(6): 1297–308.
23. Godbey WT, Hindy SB, Sherman ME, Atala A. A novel use of centrifugal force for cell seeding into porous scaffolds. Biomaterials 25, 2799, 2004.
24. Almarza AJ, Athanasiou KA. Seeding techniques and scaffolding choice for tissue engineering of temporomandibular joint disk. Tissue Eng 10, 1787, 2004.
25. Dong J, Uemura T, Kojima H, Kikuchi M, Tanaka J, Tateishi T. Application of low-pressure system to sustain in vivo bone formation in osteoblast/porous hydroxyapatite composite. Mater Sci Eng C. 2001, 17:37-43.
26. Julie C. Crockett, Michael J. Rogers, Fraser P: Bone remodelling at a glance, Journal of Cell Science 2001, 124: 991-998
27. Racquel, ZL; Calcium Phosphate-Based Osteoinductive Materials. Chem. Rev. 2008, 108: 4742-4753
28. Reday SA, Nardin M, Rey C: Behavior of human osteoblastic cells on stoichiometric hydroxyapatite and type A carbonate apatite: Role of surface energy. J Biomed Mater Res. 2000, 50(3): 353-64.
29. Steinkamp JA, Hansen KM, Crissman HA (1976) Flow microfluorometric and light-scatter measurement of nuclear and cytoplasmic size in mammalian cells. J Histochem

Cytochem 1976, 24: 292–297.

30. Smith IO, McCabe LR, Baumann MJ: MC3T3-E1 osteoblast attachment and proliferation on porous hydroxyapatite scaffolds fabricated with nanophase powder. Intl. J Nanomed 2006, 1(2): 189–94.
31. Webster TJ, Schadler LS, Siegel RW, Bizios R: Mechanisms of enhanced osteoblast adhesion on nanophase alumina involve vitronectin. Tissue Engineering 2001, 7(3): 291–301.
32. Eduardo J. Feres F, Gabriel B, Philip C: Regulation of Lysyl Oxidase by Basic Fibroblast Growth Factor in Osteoblastic MC3T3-E1 Cells. J Bio. Chem. 1996, 271: 6411–6416.
33. Fei Y, Xiao L, Doetschman T, Coffin D: Fibroblast growth factor 2 stimulation of osteoblast differentiation and bone formation is mediated by modulation of the Wnt signaling pathway. J Bio. Chem. 2011, 286(47): 40575–83.
34. FrancËoise D, JeÂrome L, Eric H, Philippe D, Joseph C, Pierre JM: Fibroblast Growth Factor-2 (FGF-2) Increases N-Cadherin Expression Through Protein Kinase C and Src-Kinase Pathways in Human Calvaria Osteoblasts. J Cellular Biochem 2001. 81: 68-81
35. Zivko M: Experimental studies on interactions between biomaterials and bone cells Biological interface of bone graft substitute materials 2011, 121: ISSN 0345-7532
36. Park KH, Kang JW, Lee E, Kim JS, Rhee Y: Melatonin promotes osteoblastic differentiation through the BMP/ERK/Wnt signaling pathways. Journal of Pineal Research 2011, 51(2): 187–94.
37. Ostrowska Z, Ziora K, Kos-Kudła B, Swietochowska E, Oświecimska J: Melatonin, the RANKL/RANK/OPG system, and bone metabolism in girls with anorexia nervosa. Endokrynol Pol. 2010, 61(1):117-23.
38. Conti A, Concon S, Hertens E, Skwarlo-Sonta K, Markowska M, Maestroni JM: Evidence for melatonin synthesis in mouse and human bone marrow cells. J Pineal Res 2000 28: 193– 202.

39. Csaba G, Barath P: The effect of pinealectomy on the parafollicular cells of the rat thyroid gland. Acta Biol 1977, 28:143– 144.

40. Tan D, Reiter RJ, Manchester LC, Yan M, El-Sawi M, Sainz RM: Chemical and physical properties and potential mechanisms: melatonin as a broad spectrum antioxidant and free radical scavenger. Current Topics in Medicinal Chemistry 2002, 2(2): 181–97.

41. Kwak EJ, Lee Y, Choi EM: Effect of magnolol on the function of osteoblastic MC3T3-E1 cells. Mediators of Inflammation 2012, 2012: 829650.

42. Lee YS, Chen X, Anderson J: Physiological concentrations of genistein stimulate the proliferation and protect against free radical-induced oxidative damage of MC3T3-E1 osteoblast-like cells. Nutrition Res 2001, 21(9): 1287–1298.

43. Hughes-Fulford, M, Li CF: The role of FGF-2 and BMP-2 in regulation of gene induction, cell proliferation and mineralization. J Orthop Surg. Res. 2011, 6: 8.

44. Takechi M., Tatehara S, Satomura, K, Fujisawa K: Effect of FGF-2 and melatonin on implant bone healing: a histomorphometric study. Journal of Materials Science. Materials in Medicine 2008, 19(8): 2949–52.

FIGURE 1

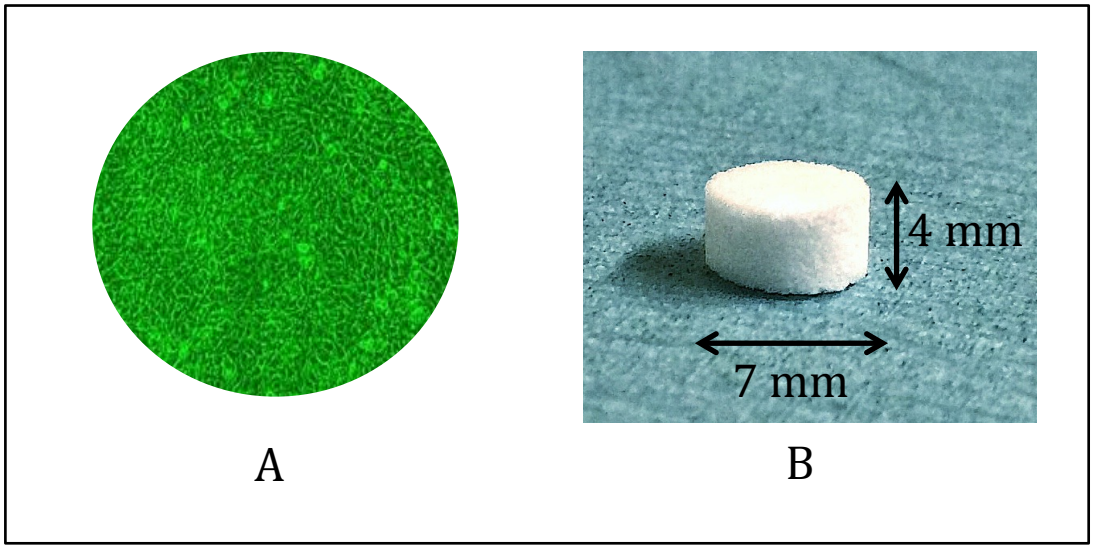

FIGURE 2

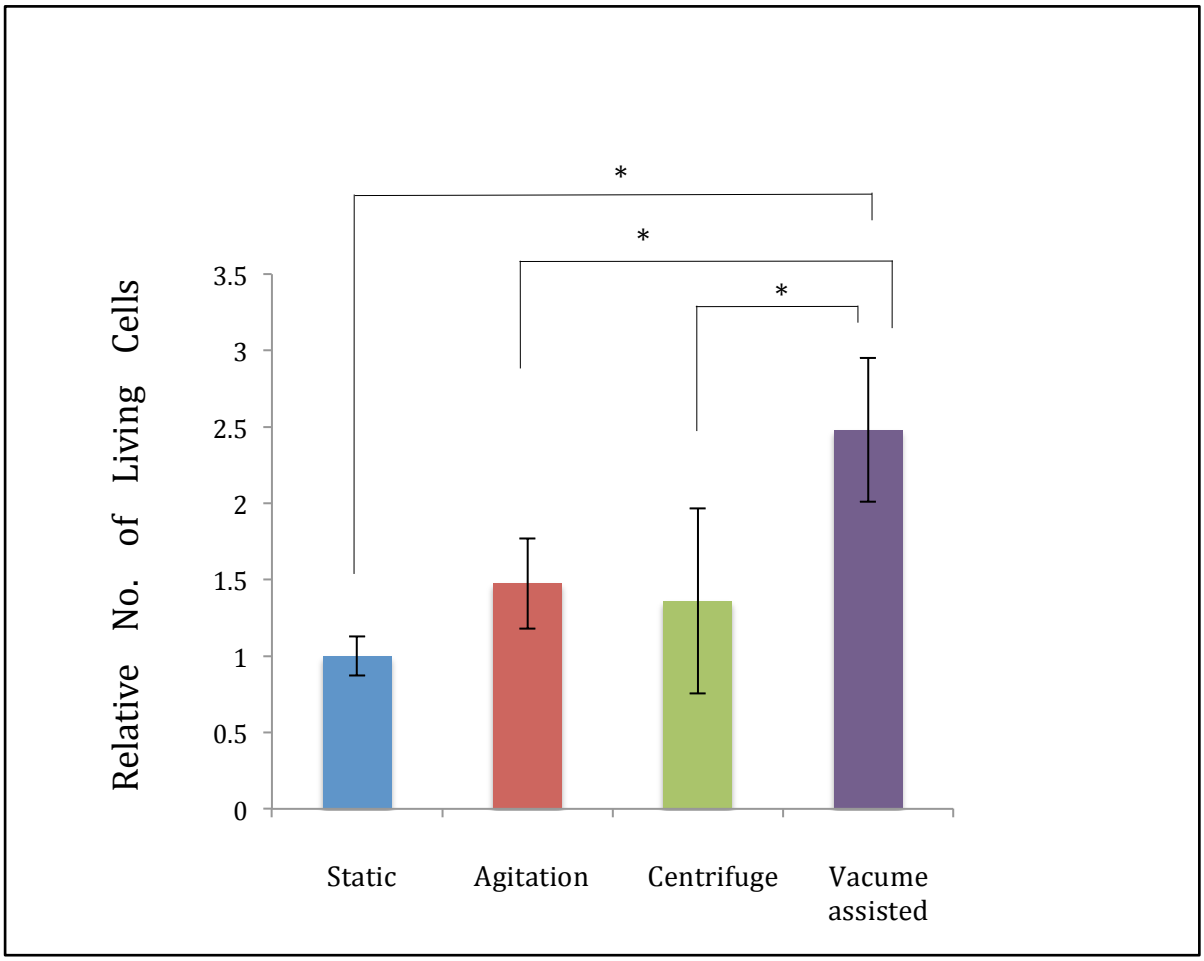
Relative No. of Living Cells
3.5
3
2.5
2
1.5
1
0.5
0
*
*
*
Static
Agitation
Centrifuge
Vacume assisted

FIGURE 3

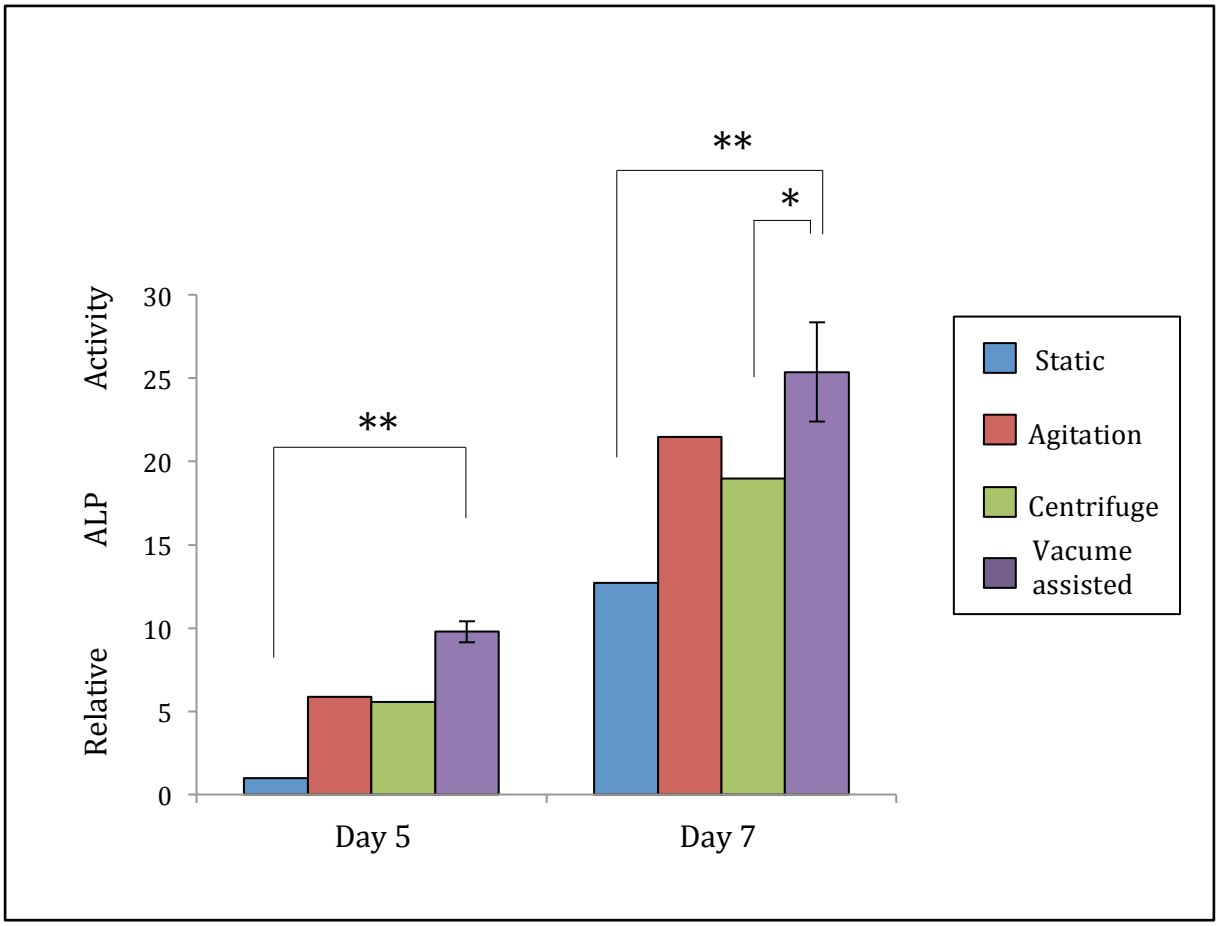
**
*
**
Relative ALP Activity
30
25
20
15
10
5
0
Day 5
Day 7
Static
Agitation
Centrifuge
Vacume assisted

FIGURE 4

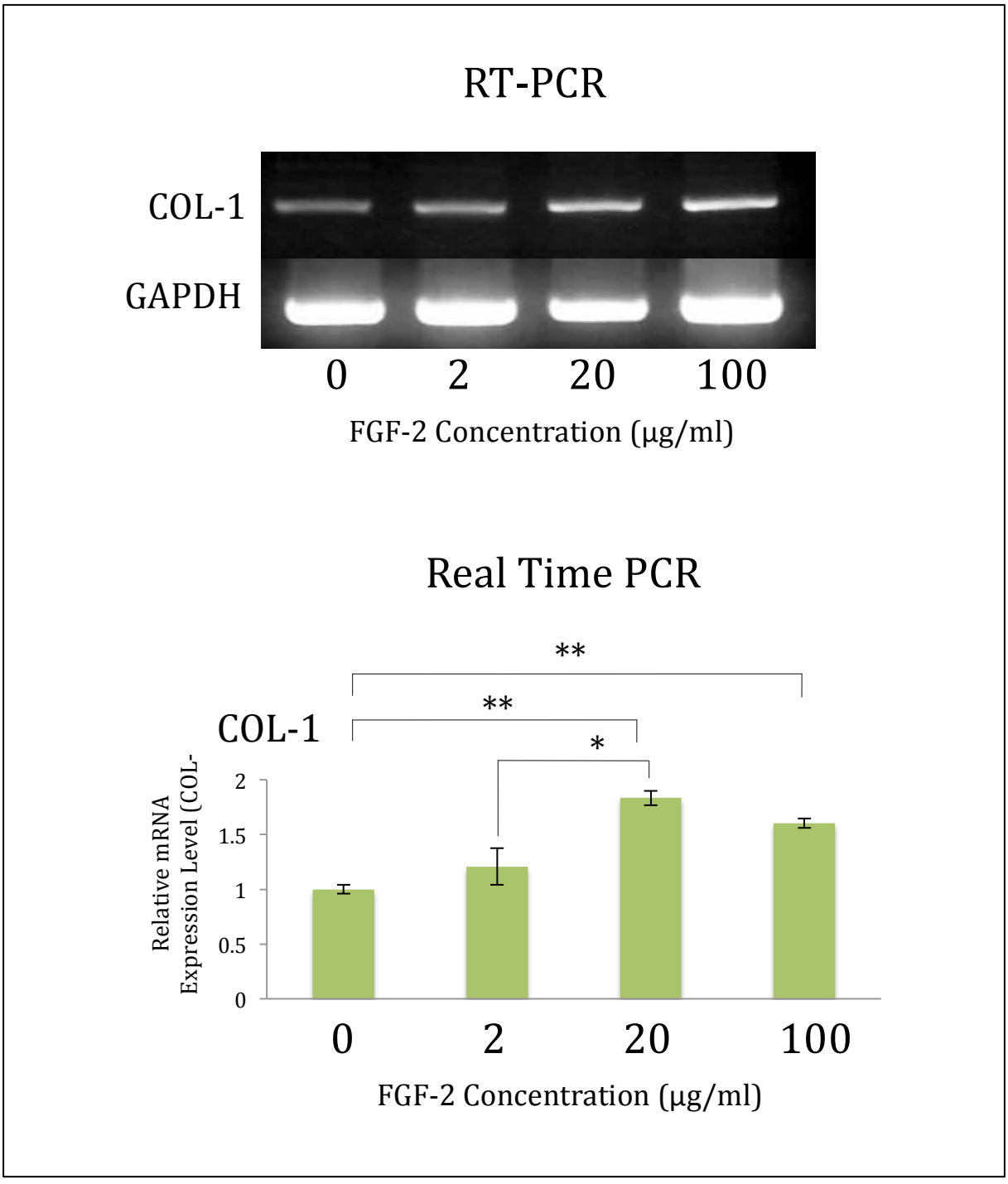
RT-PCR
COL-1
GAPDH
0
2
20
100
FGF-2 Concentration (µg/ml)
Real Time PCR
COL-1
**
**
*
Relative mRNA Expression Level (COL-
2
1.5
1
0.5
0
0
2
20
100
FGF-2 Concentration (µg/ml)

FIGURE 5

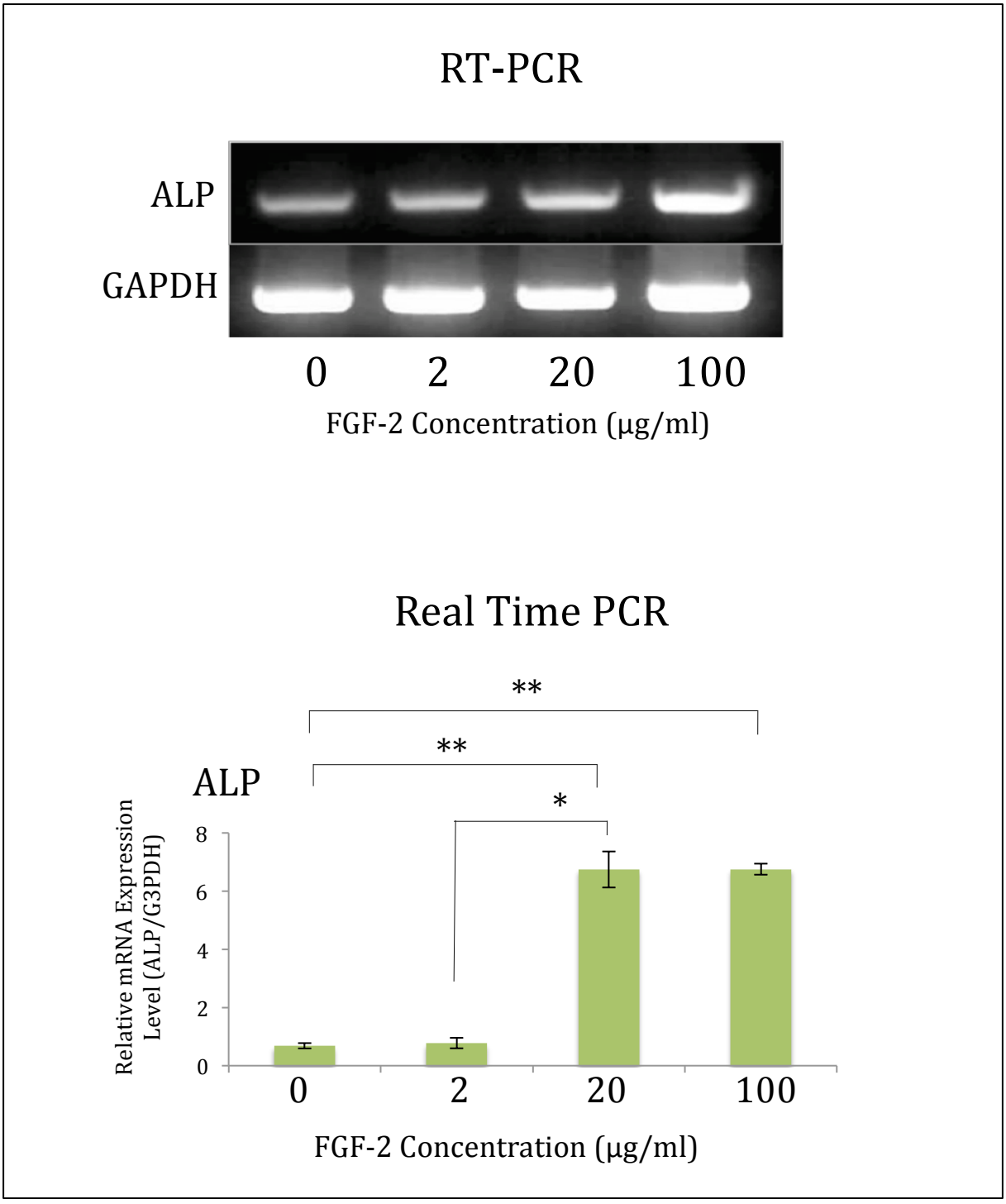
RT-PCR
ALP
GAPDH
0
2
20
100
FGF-2 Concentration (μg/ml)
Real Time PCR
**
**
*
ALP
Relative mRNA Expression Level (ALP/G3PDH)
8
6
4
2
0
0
2
20
100
FGF-2 Concentration (μg/ml)

FIGURE 6

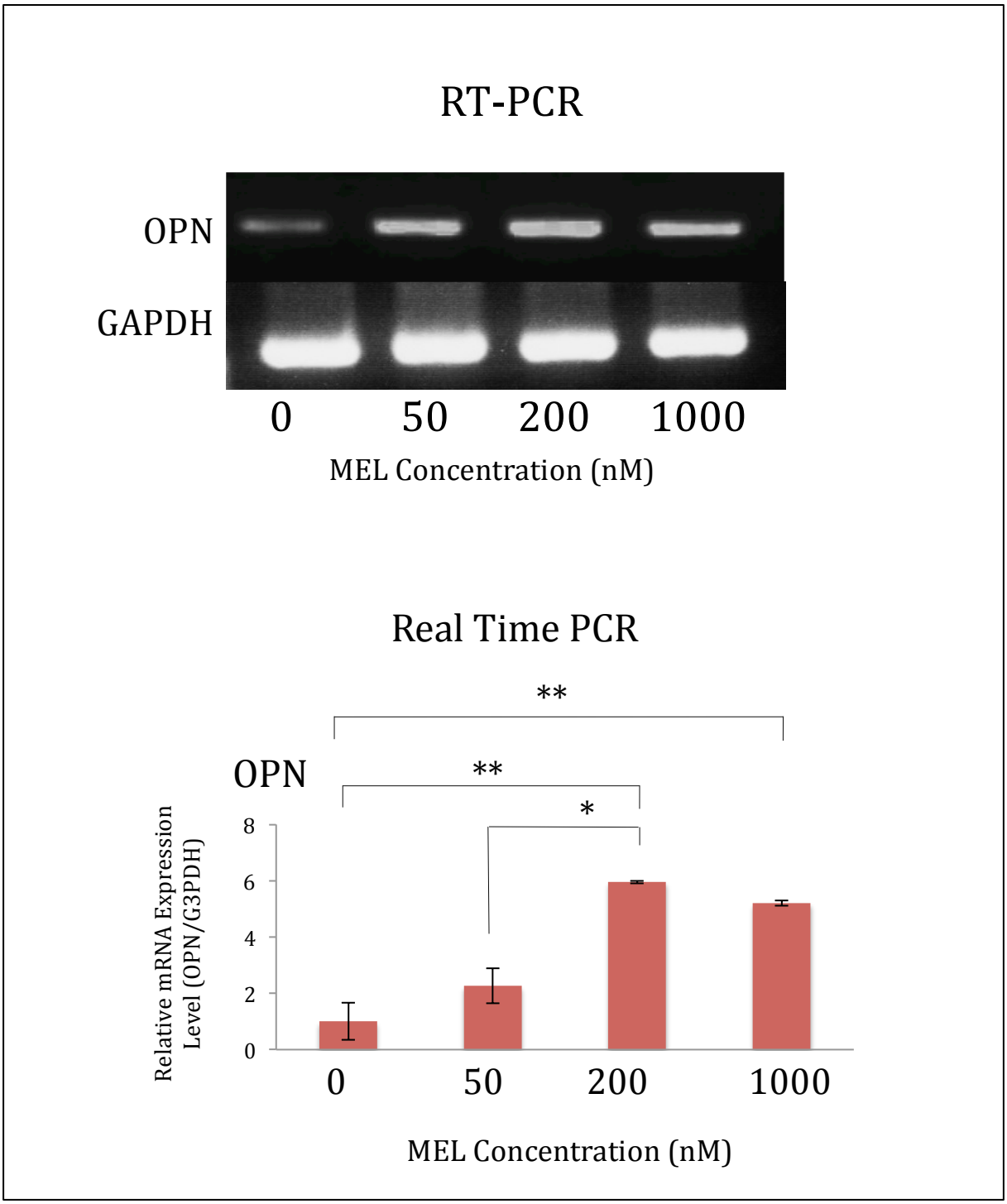
RT-PCR
OPN
GAPDH
0
50
200
1000
MEL Concentration (nM)
Real Time PCR
**
OPN
**
*
Relative mRNA Expression Level (OPN/G3PDH)
8
6
4
2
0
0
50
200
1000
MEL Concentration (nM)

FIGURE 7

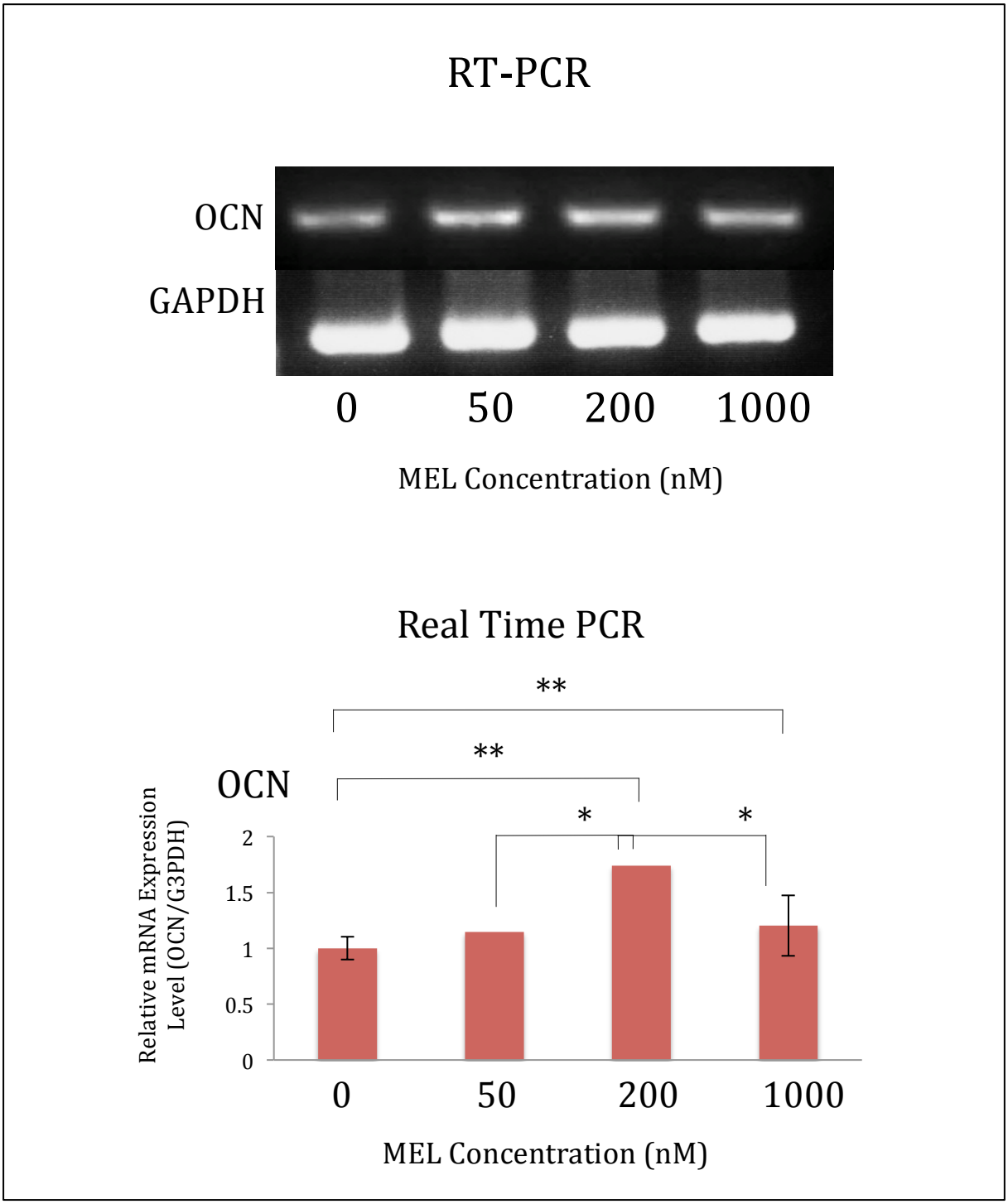
RT-PCR
OCN
GAPDH
0
50
200
1000
MEL Concentration (nM)
Real Time PCR
**
**
OCN
*
*
Relative mRNA Expression Level (OCN/G3PDH)
2
1.5
1
0.5
0
0
50
200
1000
MEL Concentration (nM)

FIGURE 8

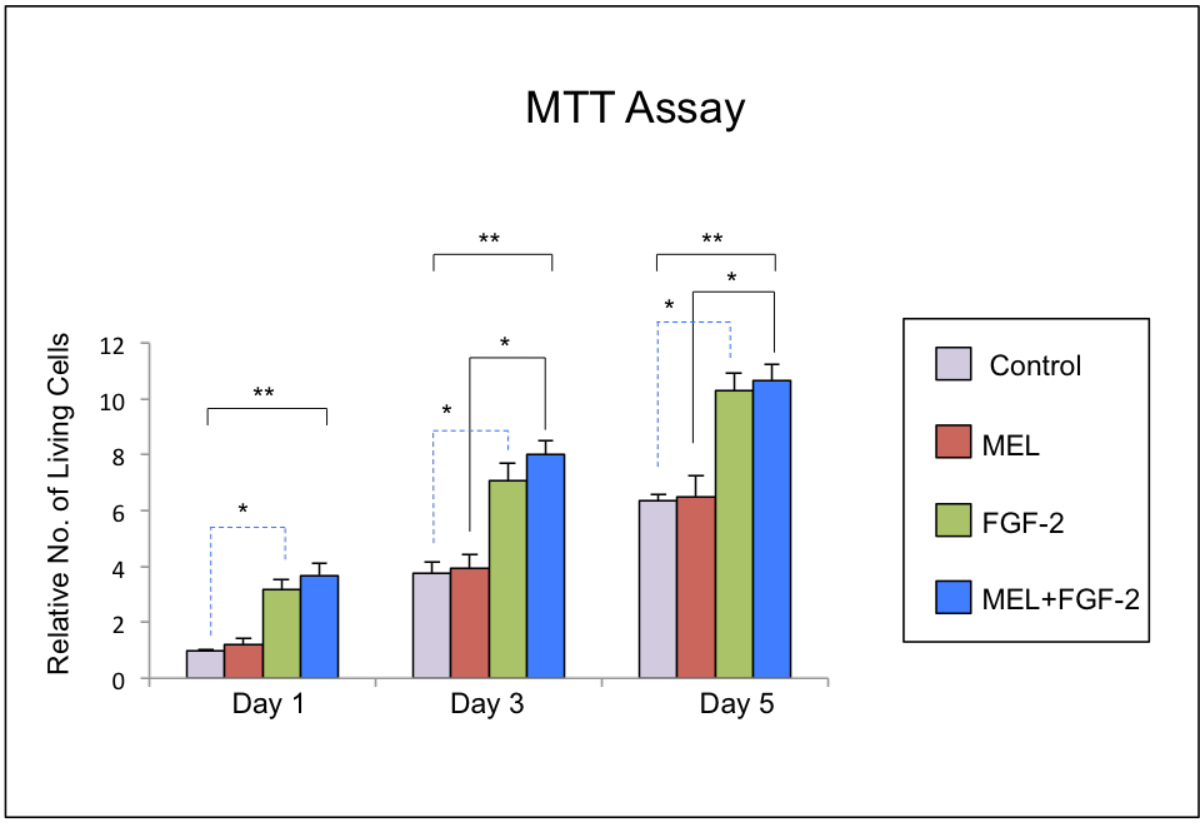
MTT Assay
Relative No. of Living Cells
0
2
4
6
8
10
12
Day 1
Day 3
Day 5
**
*
**
*
*
**
*
*
Control
MEL
FGF-2
MEL+FGF-2

FIGURE 9

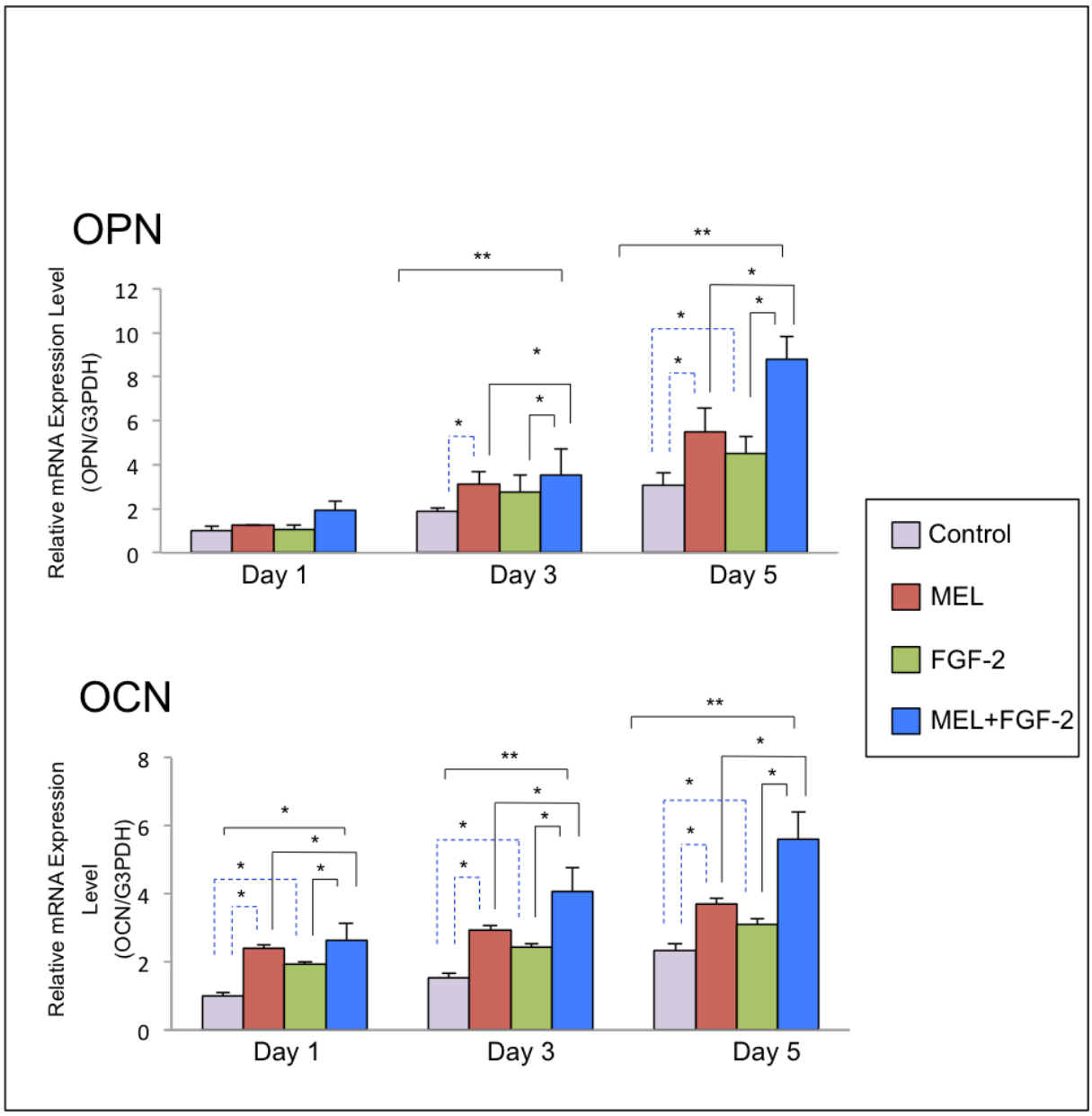
OPN
Relative mRNA Expression Level (OPN/G3PDH)
12
10
8
6
4
2
0
Day 1
Day 3
Day 5
OCN
Relative mRNA Expression Level (OCN/G3PDH)
8
6
4
2
0
Day 1
Day 3
Day 5
Control
MEL
FGF-2
MEL+FGF-2

FIGURE 10

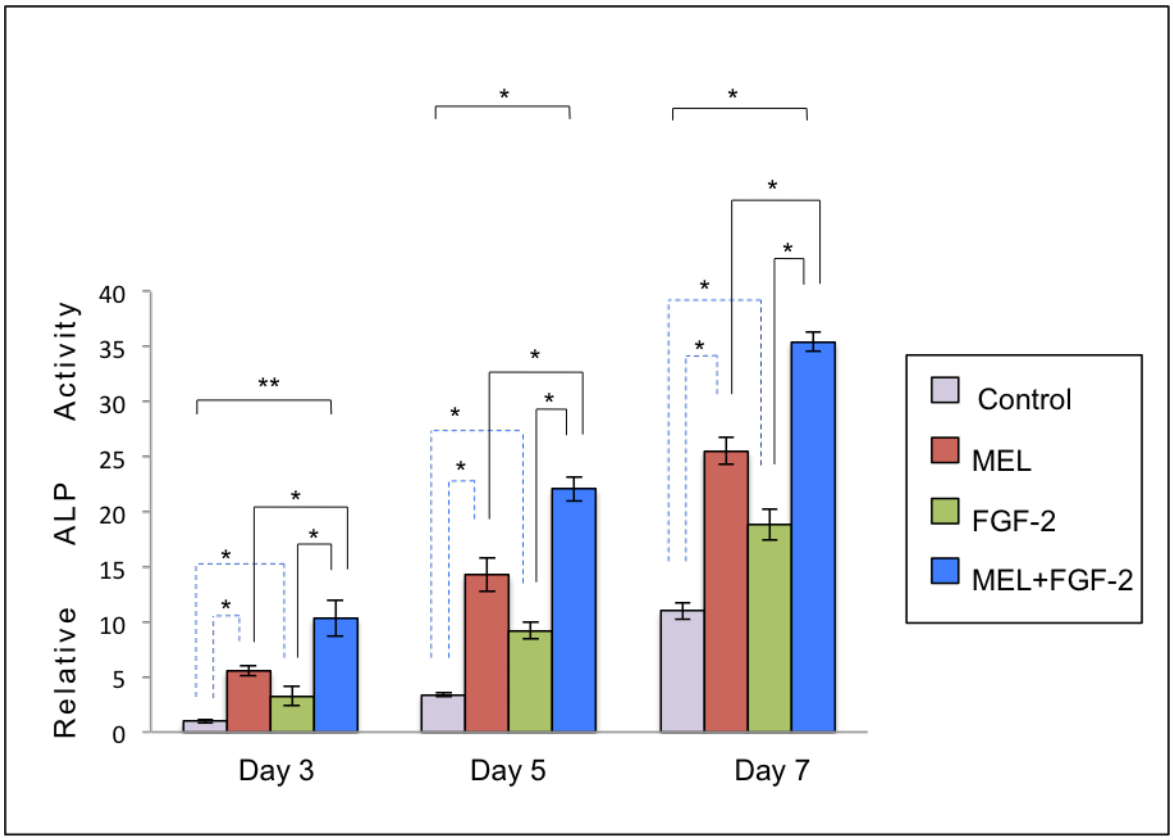
Relative ALP Activity
40
35
30
25
20
15
10
5
0
Day 3
Day 5
Day 7
Control
MEL
FGF-2
MEL+FGF-2

FIGURE 11

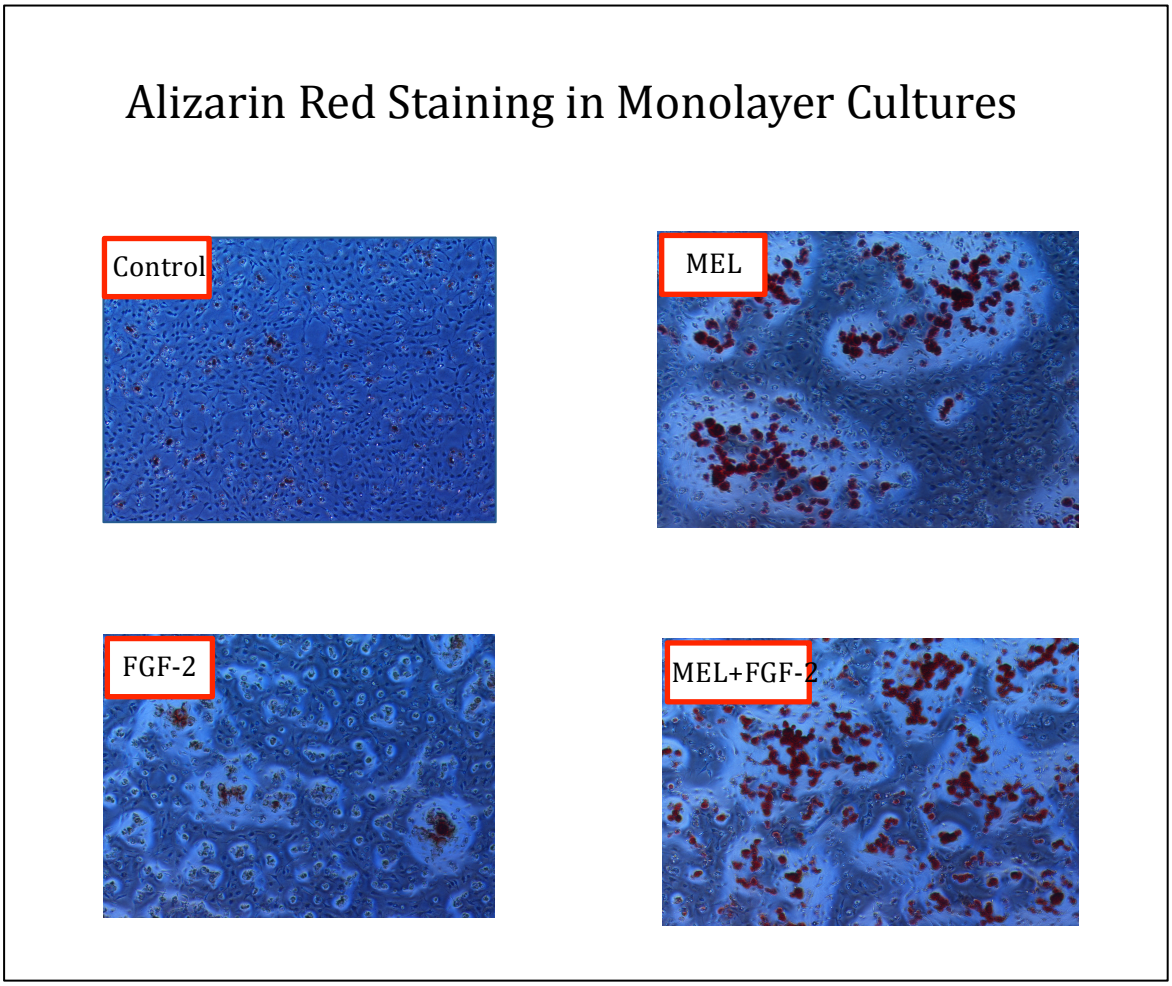
Alizarin Red Staining in Monolayer Cultures
Control
MEL
FGF-2
MEL+FGF-2

FIGURE 12

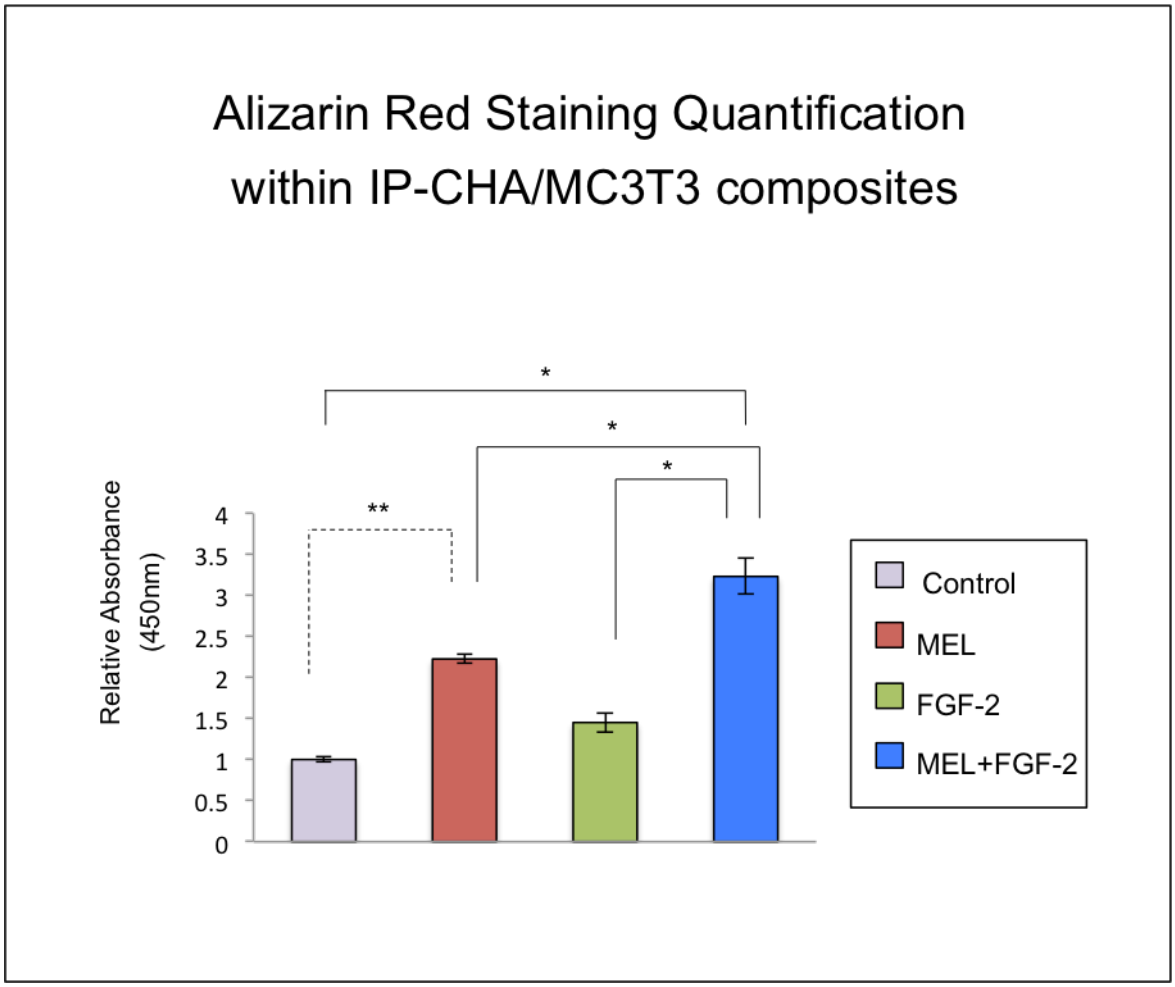
Alizarin Red Staining Quantification
within IP-CHA/MC3T3 composites
Relative Absorbance
(450nm)
4
3.5
3
2.5
2
1.5
1
0.5
0
*
*
*
**
Control
MEL
FGF-2
MEL+FGF-2

FIGURE 13

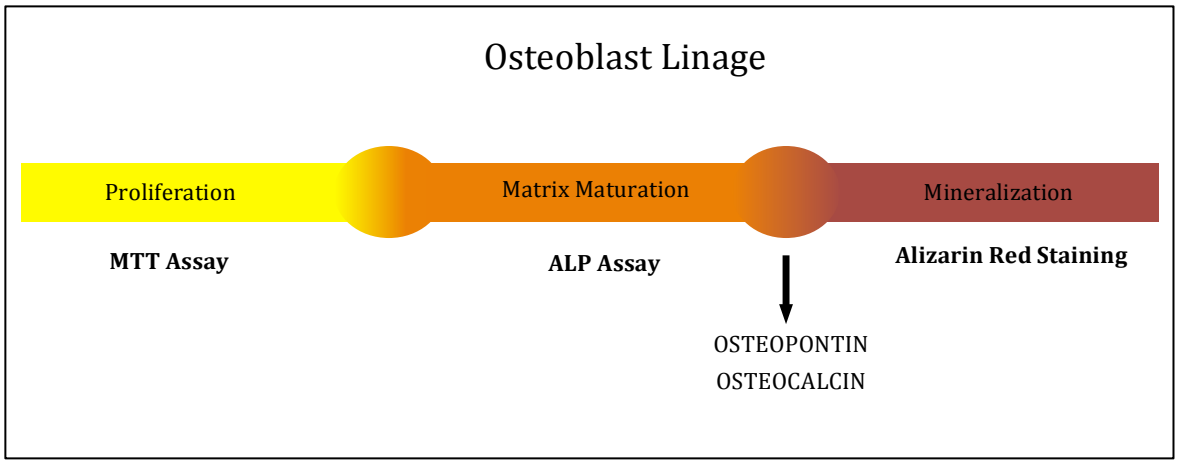
Osteoblast Linage
Proliferation
Matrix Maturation
Mineralization
MTT Assay
ALP Assay
Alizarin Red Staining
OSTEOPONTIN
OSTEOCALCIN

FIGURE LEGEND

FIGURE 1: Mouse preosteoblast cells, MC3T3-E1 (A). IP-CHA cylindrical block 7 mm in diameter, 4 mm in height (B)

FIGURE 2: Proliferation Assay. Compared to static, agitation and centrifugation, the rate of proliferation was significantly higher in cells seeded with vacume-assisted method.

FIGURE 3. From DAY 5, amongst the four methods of cell-seeding, vacume-assisted method consistently showed higher Alkaline phosphatase activity. The statistical significance was calculated by one-way ANOVA and $p<0.05$ and <0.01 were indicated by * and ** respectively.

FIGURE 4: The lowest most effective concentration of FGF-2 was 20µg/ml compared to 0 and 2µg/ml that induced COL-1 expression. Student's t-test statistical significances of $P<0.05$ and $P<0.01$ were indicated by *, ** respectively.

FIGURE 5: The lowest most effective concentration of FGF-2 was 20µg/ml compared to 0 and 2µg/ml that induced ALP expression. Student's t-test statistical significances of $P<0.05$ and $P<0.01$ were indicated by *, ** respectively.

FIGURE 6: The lowest most effective concentration of MEL was 200nM compared to 0 and 50nM that induced OPN expression. Student's t-test statistical significances of $P<0.05$ and $P<0.01$ were indicated by *, ** respectively.

FIGURE 6: The lowest most effective concentration of MEL was 200nM compared to 0 and 50nM that induced OCN expression. Student's t-test statistical significances of $P<0.05$ and $P<0.01$ were indicated by *, ** respectively.

FIGURE 8: Cell growth was significantly induced by FGF-2 compared to the control and MEL. Additionally, the combination of MEL and FGF-2 more markedly promoted the proliferation of MC3T3-E1 cells. The statistical significance was calculated by one-way ANOVA and $p<0.05$ and <0.01 were indicated by * and ** respectively.

FIGURE 9: The mRNA expression of OPN and OCN showed significant expression by independent treatment with MEL from day 3. Furthermore, the combined effect of MEL and FGF-2 was significantly greater. The statistical significance was calculated by one-way ANOVA and $p<0.05$ and <0.01 were indicated by * and ** respectively.

FIGURE 10: The Alkaline Phosphatase activity from 3 days onwards was significantly higher in cells treated with MEL. Mainly MEL induce ALP activity and the combination markedly increased ALP activity. The statistical significance was calculated by one-way ANOVA and $p<0.05$ and <0.01 were indicated by * and ** respectively.

FIGURE 11: The alizarin red staining of the monolayer cultures shows increased stains of mineralization after 2 weeks of treatment with the MEL, FGF-2, in osteogenic induction medium compared to the control. Both MEL and FGF-2 independently show signs of mineralization but the combination of MEL and FGF-2 showed more intense stains of mineralization.

FIGURE 12: The quantified values obtained from the cells cultured within IP-CHA constructs suggest the role of MEL in mineralization and the combined effect of FGF-2 and MEL positively stimulates mineralization. The statistical significance was calculated by one-way ANOVA and $p<0.05$ and <0.01 were indicated by * and ** respectively.

FIGURE 13: Schematic representation of osteoblast linage.